Title

Fluorescence-guided Surgery with a Fluorophore-conjugated Antibody to Carcinoembryonic Antigen (CEA), that Highlights the Tumor, Improves Surgical Resection and Increases Survival in Orthotopic Mouse Models of Human Pancreatic Cancer

Permalink

https://escholarship.org/uc/item/3vh383d1

Journal

Annals of Surgical Oncology, 21(4)

ISSN

1068-9265

Authors

Metildi, Cristina A
Kaushal, Sharmeela
Pu, Minya
et al.

Publication Date

2014-04-01

DOI

10.1245/s10434-014-3495-y

Peer reviewed

Fluorescence-guided Surgery with a Fluorophore-conjugated Antibody to Carcinoembryonic Antigen (CEA), that Highlights the Tumor, Improves Surgical Resection and Increases Survival in Orthotopic Mouse Models of Human Pancreatic Cancer

Cristina A. Metildi, MD[1], **Sharmeela Kaushal, PhD**[2], **Minya Pu, MA**[2], **Karen A. Messer, PhD**[2], **George A. Luiken, MD**[3], **Abdool R. Moossa, MD**[1], **Robert M. Hoffman, PhD**[1,2,4], and **Michael Bouvet, MD, FACS**[1,2,5]

[1]Department of Surgery, University of California San Diego, San Diego, CA

[2]UCSD Moores Cancer Center, La Jolla, CA

[3]OncoFluor, Inc., San Diego, CA

[4]AntiCancer, Inc., San Diego, CA

[5]San Diego VA Healthcare System, San Diego, CA

Abstract

Background—We have developed a method of distinguishing normal tissue from pancreatic cancer in vivo using fluorophore-conjugated antibody to carcinoembryonic antigen (CEA). The objective of this study was to evaluate whether fluorescence-guided surgery (FGS) with a fluorophore-conjugated antibody to CEA, to highlight the tumor, can improve surgical resection and increase disease free survival (DFS) and overall survival (OS) in orthotopic mouse models of human pancreatic cancer.

Methods—We established nude-mouse models of human pancreatic cancer with surgical orthotopic implantation of the human BxPC-3 pancreatic cancer. Orthotopic tumors were allowed to develop for 2 weeks. Mice then underwent bright-light surgery (BLS) or FGS 24 h after intravenous injection of anti-CEA-Alexa Fluor 488. Completeness of resection was assessed from postoperative imaging. Mice were followed postoperatively until premorbid to determine DFS and OS.

Results—Complete resection was achieved in 92 % of mice in the FGS group compared to 45.5 % in the BLS group ($p = 0.001$). FGS resulted in a smaller postoperative tumor burden ($p = 0.01$). Cure rates with FGS compared to BLS improved from 4.5 to 40 %, respectively ($p = 0.01$), and 1-year postoperative survival rates increased from 0 % with BLS to 28 % with FGS ($p = 0.01$).

Median DFS increased from 5 weeks with BLS to 11 weeks with FGS ($p = 0.0003$). Median OS increased from 13.5 weeks with BLS to 22 weeks with FGS ($p = 0.001$).

Conclusions—FGS resulted in greater cure rates and longer DFS and OS using a fluorophore-conjugated anti-CEA antibody. FGS has potential to improve the surgical treatment of pancreatic cancer.

Pancreatic ductal adenocarcinoma remains a lethal disease with aggressive potential and a 5-year survival of 6 %.[1] An apparent curative resection is achieved in only 10–20 % of patients, however.[2] Positive margins, defined as the presence of cancer cells in the surrounding area after surgical resection, have been associated with increased local recurrence and decreased overall survival (OS).[3–6] Therefore, complete resection of tumor is necessary to achieve cure and prolong survival in patients with pancreatic cancer.

Our laboratory has developed fluorescence-guided surgery (FGS) using patient-like orthotopic mouse models of human cancer that closely mimic patients.[7,8] We have previously demonstrated that by enhancing the surgeon's ability to distinguish tumor margins labeled with green fluorescent protein, FGS resulted in more complete resection, subsequently improving disease-free survival (DFS) and decreasing pancreatic tumor burden postoperatively in an orthotopic mouse model of human pancreatic cancer.[7,9]

In the present study, we inquired whether the more clinically-relevant approach of FGS through the use of a fluorophore-conjugated antibody against carcinoembryonic antigen (CEA), to highlight the tumor, could enhance surgical resection and improve DFS and OS in orthotopic mouse models of human pancreatic cancer. The ability to have negative margins is of particular importance in pancreatic cancer.

Methods

Cell Culture

Human BxPC-3-red fluorescent protein (RFP) pancreatic cancer cells were maintained in RPMI (Gibco-BRL, Grand Island, NY) supplemented with 10 % fetal bovine serum (Hyclone, Logan, UT).[10,11]

Antibody Conjugation

Monoclonal antibody specific for carcinoembryonic antigen (CEA) was purchased from Aragen Biosciences (Morgan Hill, CA). The antibody is an IgG monoclonal antibody to human CEA generated in murine species. The antibody was labeled with the AlexaFluor 488 or 555 Protein Labeling Kit (Molecular Probes Inc., Eugene, OR) according to the manufacturer's instructions.[12–14] Antibody and dye concentrations in the final sample were quantified using spectrophotometric absorbance with a Nanodrop ND 1000 spectrophotometer.

Animal Care

Female athymic nude mice (AntiCancer, Inc., San Diego, CA) were maintained in a barrier facility on high-efficiency particulate air-filtered racks. All surgical procedures and imaging

were performed with the animals anesthetized by intramuscular injection of 0.02 mL of a solution of 50 % ketamine, 38 % xylazine and 12 % ace-promazine maleate. All animal studies were conducted in accordance with the principles and procedures outlined in the NIH Guide for the Care and Use of Animals under assurance number A3873-01.

Orthotopic Tumor Implantation

Orthotopic human pancreatic cancer xenografts were established in nude mice by direct surgical implantation of single 1 mm^3 tumor fragments from fluorescent BxPC-3-RFP subcutaneous tumors.[15–18] The animals were anesthetized as described above. The tail of the pancreas was delivered through a small 6–10 mm transverse incision made on the left flank of the mouse. The tumor fragment was sutured to the tail of the pancreas with 8–0 nylon sutures. Upon completion, the pancreas was returned to the abdomen, and the incision was closed in two layers with 6–0 Ethibond nonabsorbable sutures (Ethicon Inc., Somerville, NJ).

Tumor Resection

A total of 73 mice were used in this experiment; 25 of them underwent FGS, another 22 mice underwent bright-light surgery (BLS), and the remaining 26 did not undergo any type of resection [14 received no treatment and 12 received 4 weeks of gemcitabine (GEM) treatment only]. Two weeks after orthotopic implantation of human pancreatic cancer, mice bearing BxPC-3-RFP tumors were randomly assigned to BLS, FGS, control (no treatment), or GEM treatment only (Fig. 1). The mice in the FGS group received tail vein injection of 75 μg anti-CEA-Alexa Fluor 488 at 24 h before planned resection of the pancreatic tumor. For both the FGS and BLS groups, at the time of surgery, mice were anesthetized as described above and their abdomens sterilized. The tail of the pancreas was delivered through a midline incision, and the exposed pancreatic tumor was imaged preoperatively with the Olympus OV-100 Small Animal Imaging System (Olympus Corp, Tokyo Japan) under both standard bright-field and fluorescence illumination.[19] Resection of the primary pancreatic tumor was performed using the MVX-10 long-working distance microscope (Olympus) under bright-light illumination for the BLS group and under fluorescence illumination through a band-pass green fluorescent protein a (GFPa) filter (excitation 460–490 nm; emission 510–550 nm) for the FGS group.[20] The GFPa band-pass filter is unable to visualize signals in the red fluorescent range and thus is capable of only visualizing green fluorescence. Postoperatively, the surgical resection bed was imaged with the OV-100 under both standard bright-field and fluorescence illumination with a GFP filter (excitation 460–490 nm, emission 510 nm long-pass) which allows the green fluorescence of the antibody and red fluorescence of the tumor to be visualized in order to assess completeness of surgical resection in both groups.

Postoperative Chemotherapy Treatment

Gemcitabine (GEM) (Gemzar, Eli Lilly) was reconstituted in phosphate-buffered saline at a concentration of 30 μg/μL. Chemotherapy was initiated in the GEM-only group ($n = 12$) 2 weeks after implantation.[10,21] All BLS and FGS mice ($n = 22$ and $n = 25$, respectively) also received adjuvant chemotherapy with GEM. Starting on postoperative day 1, mice received

150 mg/kg GEM twice weekly for 4 weeks via intraperitoneal injection. This dosing regimen was previously shown to have significant activity against RFP-expressing orthotopic pancreatic tumors without causing significant toxicity in nude mice.[10]

Longitudinal Animal Imaging of Tumor Growth and Recurrence

To assess for recurrence and to follow tumor progression postoperatively, weekly whole-body, noninvasive imaging of the mice was performed with the Olympus OV-100. The mice were followed until premorbid, at which point they were humanely sacrificed and open images were taken to evaluate primary pancreatic and metastatic tumor burden. Necropsy was performed on 1-year survivors. All mice that survived 1 year postoperatively were humanely sacrificed and their abdomens exposed for open imaging. Organs were also collected for ex vivo imaging to confirm the absence of fluorescent tumor, indicating no tumor recurrence. All images were analyzed with ImageJ software v1.440 (National Institutes of Health, Bethesda, MD). With ImageJ software, the intensity of fluorescence signal per pixel can be measured. With a set scale, the area of fluorescence can be calculated.

Data Processing and Statistical Analysis

SAS v9.2 (SAS Institute, Cary, NC) or R v2.15.2 was used for statistical analyses. Continuous variables (preoperative tumor burden, postoperative tumor burden, percentage tumor burden reduction) are described by mean ± standard error. The normality of the variables was assessed by visual inspection of histograms and normal Q–Q plots. A Welch's *t* test or Wilcoxon rank sum test was used to compare two groups, as appropriate. Pearson's correlation was used to explore the association between two continuous variables. Categorical variables (complete resection, recurrence, cure, and 1-year survival) were expressed as counts and percentages. Tests of significance used Fisher's exact test. To adjust for a factor that may affect binary outcomes, logistic regression analysis was performed. We compared OS and DFS between treatment groups by a log rank test. Median survival time and their 95 % confidence intervals (CIs) were calculated using the linear confidence interval method. We reported $+\infty$ for the upper bound of the interval if it could not be estimated. Hazard ratios (HRs) with their 95 % CIs were estimated by Cox proportional hazard models. The PH assumption was assessed by Schoenfeld residuals.[22] A two-sided *p* value of   0.05 was considered statistically significant for all comparisons.

Results

Primary Tumor Resection

The first aim was to evaluate the efficacy of a green fluorophore-conjugated anti-carcinoembryonic antigen (CEA) antibody to fluorescently label the BxPC-3 tumor for enhanced detection to improve surgical resection of pancreatic cancer under fluorescence guidance. The experimental outline is depicted in Fig. 1. There was no significant difference in preoperative tumor burden between the two surgical groups ($p = 0.170$). The mean preoperative tumor burden for the FGS group was 6.50 ± 0.601 versus 5.11 ± 0.813 mm^2 for the BLS group (Supplemental Fig. 1).

The anti-CEA-Alexa Fluor 488 antibody was very sensitive and specific in labeling CEA-expressing pancreatic cancer in the mouse models. AlexaFluor 488 was visible under the GFPa filter, while the RFP-expressing tumor was visible under the RFP filter. The GFP filter (excitation 460–490 nm; emission 510 nm long pass) allows simultaneous visualization of both the green antibody and the red fluorescent protein-expressing tumor, giving off a yellow color seen in the GFP+RFP image of Fig. 2. The high correlation between red and green fluorescence (Pearson correlation 0.83, $p < 0.001$) indicates that the antibody can accurately bind and label the CEA-expressing pancreatic cancer for proper delineation of tumor margins for surgical navigation. Regarding nonspecific staining, we used RFP-expressing tumors to be sure the green fluorescing anti-CEA antibody effectively labeled the tumor by imaging both labels. It is possible that the small deposits of tumor shown in Fig. 2 were not detected by the RFP filter used (emission 570–623 nm). In future experiments, spectral separation will be used to more sensitively detect both labels.

Comparing the two groups, the mean postoperative tumor burden in mice from the FGS group (0.0003 ± 0.0003 mm^2) was significantly less than in the BLS group (0.1042 ± 0.036 mm^2; $p = 0.009$) (Supplemental Fig. 2). Moreover, under FGS, the reduced tumor burden was achieved without compromising normal pancreatic tissue or resulting in extensive organ removal. On average, 99.99 % of tumor burden was reduced under fluorescence guidance compared to 96.89 % under standard white light ($p = 0.02$). With the enhanced precision of FGS, greater preservation of the pancreas was possible without compromising surgical resection of the tumor. Furthermore, FGS improved complete resection rates from 10 of 22 (45.5 %) in the BLS group to 23 of 25 (92 %) in the FGS group ($p = 0.001$) (Table 1).

Cure and 1-Year Survival

The second aim of this study was to investigate whether FGS improved recurrence, rate of cure, and 1-year survival after resection compared to BLS. Cure was defined by the absence of tumor at time of death or termination as long as the mouse survived longer than 12 weeks postoperatively. As shown in Table 1, there was a significant increase in the cure rate from 4.5 % in the BLS group to 40 % in the FGS group ($p = 0.01$). The increase was still statistically significant with adjustment for preoperative tumor burden ($p = 0.007$), assessed by a logistic regression model. FGS also afforded significantly higher 1-year survival rates (defined as alive at 1 year postoperatively) compared to BLS. No mice survived to 1 year in the BLS group, compared to 7 of 25 (28 %) alive 1 year postoperatively with FGS ($p = 0.01$). Notably, these mice were assessed with open and ex vivo imaging 1 year postoperatively and found to be free of tumor (Table 1). An exact logistic regression model showed a significant difference remains when preoperative tumor burden was adjusted for ($p = 0.007$).

DFS and OS

The mice were followed with weekly noninvasive whole-body imaging to assess for recurrence and to follow tumor progression. Mice were followed until criteria for premorbidity were met, at which time the mice were humanely sacrificed and overall length of survival (OS) in weeks was documented. DFS was documented as the earliest point in the postoperative period that tumor was visualized by weekly whole-body imaging. We

compared DFS between the two surgery groups and OS among the four treatment groups. Survival estimates along with 95 % CIs are presented in Supplemental Table 1.

FGS significantly lengthened DFS ($p < 0.001$), as demonstrated by the Kaplan–Meier survival curves in Fig. 3. Overall, mice that underwent FGS experienced a median DFS of 11 weeks (95 % CI 7, 40), compared with 5 weeks in the BLS group (95 % CI 4, 6) (Supplemental Table 2). A Cox proportional hazard model, adjusting for preoperative tumor burden, also showed reduced risk of recurrence or death in the FGS group compared to BLS (HR 0.27, 95 % CI 0.13, 0.54, $p < 0.001$).

OS differed among the four treatment groups, with FGS+GEM resulting in longer survival compared to BLS+GEM (HR 0.33, 95 % CI 0.16, 0.64, $p = 0.001$) (Fig. 4). Treatment with GEM only or with BLS and adjuvant GEM did not provide the mice with any significant survival advantage over the control mice (no treatment group) (HR 1.05 comparing no treatment vs. BLS+GEM, 95 % CI 0.53, 2.06, $p = 0.89$; and HR 0.93 comparing GEM alone vs. no treatment, 95 % CI 0.43, 2.02, $p = 0.86$). Median OS remained low at 14 weeks (95 % CI 10, 17) for the control group as well as the GEM-only group at 15 weeks (95 % CI 11, 20). We previously showed that another pancreatic cancer cell line, MiaPaCa-2, had in vivo sensitivity to GEM.[10] Therefore, in this study, we used a similar dosing scheme, but the above result suggests that the BxPC-3 may not be as sensitive to GEM as MiaPaCa-2. However, a significant increase in median OS was achieved in mice in the FGS+GEM group (22 weeks; 95 % CI 14, $+\infty$) compared to the BLS+GEM group (13.5 weeks; 95 % CI 10, 16). It was noted that because two BLS mice and five FGS mice died within the first 4 weeks of GEM treatment, OS rates were lower in the two surgical groups for the first few weeks, and the OS curves consequently crossed one another (Fig. 4). In spite of this, the Cox proportional hazard assumption was not significantly violated (p 0.07), suggesting that this method is an appropriate analytical technique.

Discussion

A number of different methods have been used to label tumors for FGS. One example is the use of activatable probes that rely on high tumor tissue enzymatic activity or the acidic pH in lysosomes.[23,24] Other examples include the use of replication-competent adenovirus engineered to express GFP in the presence of activated telomerase or by targeting rapidly replicating cells with the oncolytic herpes simplex-1 virus, NV1066.[25–28] Furthermore, there has been interest in using fluorophore-conjugated antibodies to unique surface markers expressed by individual tumor types.[12,14, 29,30] These methods have all shown promising capabilities to label tumor for enhanced detection and subsequent resection under fluorescence-guidance, leading to improved DFS and OS in mouse models of cancer.

Clinical trials of FGS include the use of the metabolite 5-aminolevulinic acid (5-ALA), a precursor of hemoglobin that results in an accumulation of fluorescent porphyrins within malignant glioma. With a modified neurosurgical microscope, surgeons could visualize porphyrin fluorescence in glioma, resulting in more complete resections ipatients undergoing FGS.[31] Another example is indocyanine green (ICG), a nontoxic compound that exhibits maximum near-infrared fluorescence (NIRF) when stimulated at 780 nm.[31] Recent

technological developments in NIRF imaging have been used in investigational human studies for mapping lymphatic vasculature for intraoperative sentinel lymph node detection for cancer staging and intraoperative identification of certain solid tumors as well as intraoperative assessment of tissue perfusion in reconstructive surgery via NIRF angiography using ICG.[32–40] More recently, use of ICG has been evaluated in fluorescence cholangiography for biliary-tree delineation during laparoscopic cholecystectomy to reduce morbid complications of bile duct injuries.[34,41,42] However, ICG cannot be conjugated to tumor-specific targets and so cannot specifically label tumors. In addition, its fluorescent properties are less effective than other emerging dyes.[43]

Our group has previously described the use of conjugated monoclonal antibodies specific for either CA19-9 or CEA to successfully deliver green fluorophores for labeling of human pancreatic and colon cancers in nude mice.[12,29] The fluorescence labeling of tumors made them visible under fluorescence lighting when they were not visible under bright light. Furthermore, fluorophore-conjugated anti-CEA antibodies improved the accuracy and diagnostic yield of staging laparoscopy in orthotopic and carcinomatosis mouse models of pancreatic cancer.[14]

In the present study of FGS in an orthotopic mouse model of pancreatic cancer, anti-CEA antibody was used since up to 98 % of pancreatic ductal adenocarcinomas express CEA, making our approach translatable.[44] Indeed, labeling with BxPC-3 was similar to a patient-derived orthotopic xenografts (PDOX), indicating that patient pancreatic tumors should be brightly labeled with this antibody.[45] Providing surgeons with a more objective way of delineating tumor from normal tissue with fluorescent probes specific for the tumor may improve the curative potential of surgery in these patients.

In conclusion, in this study in an orthotopic mouse model of pancreatic cancer, we demonstrated that FGS with fluorophore-conjugated antibodies improved surgical outcomes, reduced recurrence rates, and increased cure rates leading to improved 1-year survival rates. In order to accurately mimic the clinical situation, adjuvant GEM was also administered after FGS. With improved surgical resection of primary pancreatic cancer, FGS extended DFS and OS. The results of the present study provide a highly translatable protocol to the clinic for FGS of pancreatic cancer with an expectation of significant improvements in outcome.

Supplementary Material

Refer to Web version on PubMed Central for supplementary material.

Acknowledgments

References

1. Siegel R, Naishadham D, Jemal A. Cancer statistics, 2013. CA Cancer J Clin. 2013; 63:11–30. [PubMed: 23335087]

2. Stefanidis D, Grove KD, Schwesinger WH, Thomas CR Jr. The current role of staging laparoscopy for adenocarcinoma of the pancreas: a review. Ann Oncol. 2006; 17:189–99. [PubMed: 16236756]

3. Adham M, Jaeck D, Le Borgne J, et al. Long-term survival (5–20 years) after pancreatectomy for pancreatic ductal adenocarcinoma: a series of 30 patients collected from 3 institutions. Pancreas. 2008; 37:352–7. [PubMed: 18665012]

4. Conlon KC, Klimstra DS, Brennan MF. Long-term survival after curative resection for pancreatic ductal adenocarcinoma. Clinicopathologic analysis of 5-year survivors. Ann Surg. 1996; 223:273–9. [PubMed: 8604907]

5. Shimada K, Sakamoto Y, Nara S, Esaki M, Kosuge T, Hiraoka N. Analysis of 5-year survivors after a macroscopic curative pancreatectomy for invasive ductal adenocarcinoma. World J Surg. 2010; 34:1908–15. [PubMed: 20376443]

6. Yeo CJ, Cameron JL, Lillemoe KD, et al. Pancreaticoduodenectomy for cancer of the head of the pancreas. 201 patients. Ann Surg. 1995; 221:721–31. [PubMed: 7794076]

7. Metildi CA, Kaushal S, Hardamon CR, et al. Fluorescence-guided surgery allows for more complete resection of pancreatic cancer, resulting in longer disease-free survival compared with standard surgery in orthotopic mouse models. J Am Coll Surg. 2012; 215:126–35. [PubMed: 22632917]

8. Metildi CA, Kaushal S, Snyder CS, Hoffman RM, Bouvet M. Fluorescence-guided surgery of human colon cancer increases complete resection resulting in cures in an orthotopic nude mouse model. J Surg Res. 2013; 179:87–93. [PubMed: 23079571]

9. Bouvet M, Hoffman RM. Glowing tumors make for better detection and resection. Sci Transl Med. 2011; 3:110fs10.

10. Katz MH, Takimoto S, Spivack D, Moossa AR, Hoffman RM, Bouvet M. A novel red fluorescent protein orthotopic pancreatic cancer model for the preclinical evaluation of chemotherapeutics. J Surg Res. 2003; 113:151–60. [PubMed: 12943825]

11. Katz MH, Takimoto S, Spivack D, Moossa AR, Hoffman RM, Bouvet M. An imageable highly metastatic orthotopic red fluorescent protein model of pancreatic cancer. Clin Exp Metastasis. 2004; 21:7–12. [PubMed: 15065597]

12. Kaushal S, McElroy MK, Luiken GA, et al. Fluorophore-conjugated anti-CEA antibody for the intraoperative imaging of pancreatic and colorectal cancer. J Gastrointest Surg. 2008; 12:1938–50. [PubMed: 18665430]

13. Metildi CA, Kaushal S, Lee C, et al. An LED light source and novel fluorophore combinations improve fluorescence laparoscopic detection of metastatic pancreatic cancer in orthotopic mouse models. J Am Coll Surg. 2012; 214:997–1007. e2. [PubMed: 22542065]

14. Tran Cao HS, Kaushal S, Metildi CA, et al. Tumor-specific fluorescence antibody imaging enables accurate staging laparoscopy in an orthotopic model of pancreatic cancer. Hepatogastroenterology. 2012; 59:1994–9. [PubMed: 22369743]

15. Bouvet M, Wang J, Nardin SR, et al. Real-time optical imaging of primary tumor growth and multiple metastatic events in a pancreatic cancer orthotopic model. Cancer Res. 2002; 62:1534–40. [PubMed: 11888932]

16. Bouvet M, Yang M, Nardin S, et al. Chronologically-specific metastatic targeting of human pancreatic tumors in orthotopic models. Clin Exp Metastasis. 2000; 18:213–8. [PubMed: 11315094]

17. Fu X, Guadagni F, Hoffman RM, et al. A metastatic nude-mouse model of human pancreatic cancer constructed orthotopically with histologically intact patient specimens. Proc Natl Acad Sci USA. 1992; 89:5645–9. [PubMed: 1608975]

18. Furukawa T, Kubota T, Watanabe M, Kitajima M, Hoffman RM. A novel "patient-like" treatment model of human pancreatic cancer constructed using orthotopic transplantation of histologically intact human tumor tissue in nude mice. Cancer Res. 1993; 53:3070–2. [PubMed: 8319214]

19. Yamauchi K, Yang M, Jiang P, et al. Development of real-time subcellular dynamic multicolor imaging of cancer-cell trafficking in live mice with a variable-magnification whole-mouse imaging system. Cancer Res. 2006; 66:4208–14. [PubMed: 16618743]

20. Kimura H, Hayashi K, Yamauchi K, et al. Real-time imaging of single cancer-cell dynamics of lung metastasis. J Cell Biochem. 2010; 109:58–64. [PubMed: 19911396]

21. Tran Cao HS, Bouvet M, Kaushal S, et al. Metronomic gemcitabine in combination with sunitinib inhibits multisite metastasis and increases survival in an orthotopic model of pancreatic cancer. Mol Cancer Ther. 2010; 9:2068–78. [PubMed: 20606044]

22. Grambsch P, Louis TA, Bostick RM, et al. Statistical analysis of proliferative index data in clinical trials. Stat Med. 1994; 13:1619–34. [PubMed: 7973238]

23. Nguyen QT, Olson ES, Aguilera TA, et al. Surgery with molecular fluorescence imaging using activatable cell-penetrating peptides decreases residual cancer and improves survival. Proc Natl Acad Sci USA. 2010; 107:4317–22. [PubMed: 20160097]

24. Urano Y, Asanuma D, Hama Y, et al. Selective molecular imaging of viable cancer cells with pH-activatable fluorescence probes. Nat Med. 2009; 15:104–9. [PubMed: 19029979]

25. Kishimoto H, Kojima T, Watanabe Y, et al. In vivo imaging of lymph node metastasis with telomerase-specific replication selective adenovirus. Nat Med. 2006; 12:1213–9. [PubMed: 17013385]

26. Kishimoto H, Zhao M, Hayashi K, et al. In vivo internal tumor illumination by telomerase-dependent adenoviral GFP for precise surgical navigation. Proc Natl Acad Sci USA. 2009; 106:14514–7. [PubMed: 19706537]

27. Adusumilli PS, Stiles BM, Chan MK, et al. Real-time diagnostic imaging of tumors and metastases by use of a replication-competent herpes vector to facilitate minimally invasive oncological surgery. FASEB J. 2006; 20:726–8. [PubMed: 16467372]

28. Stiles BM, Adusumilli PS, Bhargava A, et al. Minimally invasive localization of oncolytic herpes simplex viral therapy of metastatic pleural cancer. Cancer Gene Ther. 2006; 13:53–64. [PubMed: 16037824]

29. McElroy M, Kaushal S, Luiken GA, et al. Imaging of primary and metastatic pancreatic cancer using a fluorophore-conjugated anti-CA19-9 antibody for surgical navigation. World J Surg. 2008; 32:1057–66. [PubMed: 18264829]

30. van Dam GM, Themelis G, Crane LM, et al. Intraoperative tumor-specific fluorescence imaging in ovarian cancer by folate receptor-alpha targeting: first in-human results. Nat Med. 2011; 17:1315–9. [PubMed: 21926976]

31. Stummer W, Pichlmeier U, Meinel T, Wiestler OD, Zanella F, Reulen HJ. Fluorescence-guided surgery with 5-aminolevulinic acid for resection of malignant glioma: a randomised controlled multicentre phase III trial. Lancet Oncol. 2006; 7:392–401. [PubMed: 16648043]

32. Hirche C, Mohr Z, Kneif S, et al. Ultrastaging of colon cancer by sentinel node biopsy using fluorescence navigation with indocyanine green. Int J Colorectal Dis. 2012; 27:319–24. [PubMed: 21912878]

33. Hirche C, Mohr Z, Kneif S, Murawa D, Hunerbein M. High rate of solitary sentinel node metastases identification by fluorescence-guided lymphatic imaging in breast cancer. J Surg Oncol. 2012; 105:162–6. [PubMed: 21882198]

34. Schaafsma BE, Mieog JS, Hutteman M, et al. The clinical use of indocyanine green as a near-infrared fluorescent contrast agent for image-guided oncologic surgery. J Surg Oncol. 2011; 104:323–32. [PubMed: 21495033]

35. Troyan SL, Kianzad V, Gibbs-Strauss SL, et al. The FLARE intraoperative near-infrared fluorescence imaging system: a first in-human clinical trial in breast cancer sentinel lymph node mapping. Ann Surg Oncol. 2009; 16:2943–52. [PubMed: 19582506]

36. Yamashita S, Tokuishi K, Miyawaki M, et al. Sentinel node navigation surgery by thoracoscopic fluorescence imaging system and molecular examination in non-small cell lung cancer. Ann Surg Oncol. 2012; 19:728–33. [PubMed: 22101727]

37. Hagen A, Grosenick D, Macdonald R, et al. Late-fluorescence mammography assesses tumor capillary permeability and differentiates malignant from benign lesions. Opt Express. 2009; 17:17016–33. [PubMed: 19770920]

38. Ishizawa T, Fukushima N, Shibahara J, et al. Real-time identification of liver cancers by using indocyanine green fluorescent imaging. Cancer. 2009; 115:2491–504. [PubMed: 19326450]

39. Watanabe M, Tsunoda A, Narita K, Kusano M, Miwa M. Colonic tattooing using fluorescence imaging with light-emitting diodeactivated indocyanine green: a feasibility study. Surg Today. 2009; 39:214–8. [PubMed: 19280280]

40. Lee BT, Matsui A, Hutteman M, et al. Intraoperative near-infrared fluorescence imaging in perforator flap reconstruction: current research and early clinical experience. J Reconstr Microsurg. 2010; 26:59–65. [PubMed: 20027541]

41. Schols RM, Bouvy ND, Masclee AA, van Dam RM, Dejong CH, Stassen LP. Fluorescence cholangiography during laparoscopic cholecystectomy: a feasibility study on early biliary tract delineation. Surg Endosc. 2013; 27:1530–6. [PubMed: 23076461]

42. Spinoglio G, Priora F, Bianchi PP, et al. Real-time near-infrared (NIR) fluorescent cholangiography in single-site robotic cholecystectomy (SSRC): a single-institutional prospective study. Surg Endosc. 2013; 27:2156–62. [PubMed: 23271272]

43. Sevick-Muraca EM. Translation of near-infrared fluorescence imaging technologies: emerging clinical applications. Annu Rev Med. 2012; 63:217–31. [PubMed: 22034868]

44. Yamaguchi K, Enjoji M, Tsuneyoshi M. Pancreatoduodenal carcinoma: a clinicopathologic study of 304 patients and immunohistochemical observation for CEA and CA19-9. J Surg Oncol. 1991; 47:148–54. [PubMed: 2072697]

45. Hiroshima Y, Maawy A, Sato S, et al. Hand-held high resolution fluorescence imaging system for fluorescence-guided surgery of patient and cell-line pancreatic tumors growing orthotopically in nude mice. J Surg Res. 201310.1016/j.jss.2013.11.1083
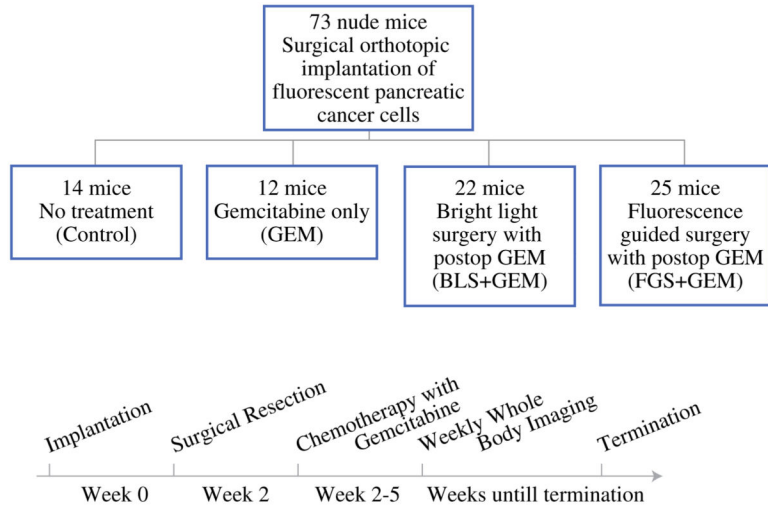
Fig. 1.

Study schema. Two weeks after implantation, the mice were randomized to 1 of 4 treatment groups: control (no treatment), GEM only, BLS with adjuvant GEM, or FGS with adjuvant GEM. Tumors were resected using the MVX-10 microscope. Starting on postoperative day 0, all mice from each surgical arm underwent 4 weeks of GEM treatment. GEM treatment was started 2 weeks after implantation of tumor fragments in the GEM-only group and continued for 4 weeks. All 73 mice were followed postoperatively and imaged weekly using the OV-100. When premorbid, the mice were humanely sacrificed for open imaging
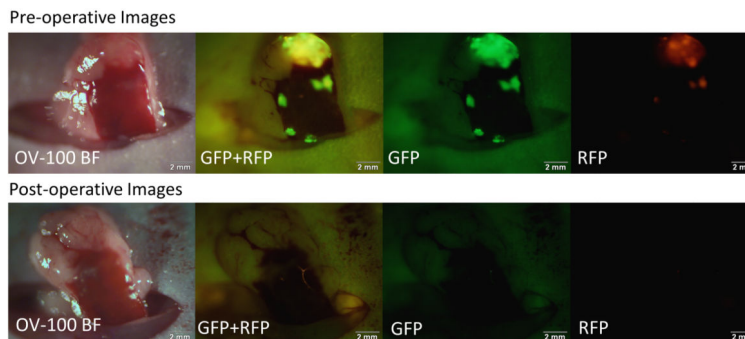
Fig. 2.
Pre- and postoperative tumor burden. Representative OV-100 images are shown of a mouse from the FGS group with the tail of the pancreas and spleen delivered through a midline incision. From *left* to *right*, images were taken under bright field (BF), or using the following filters: a GFP filter (excitation 460–490 nm, emission 510 nm long-pass); a GFPa filter (excitation 460–490 nm, emission 510–550 nm); and an RFP filter (excitation 535–555 nm, emission 570–623 nm). With the GFPa filter, only the AlexaFluor 488 bound to CEA is visualized. The RFP filter only permits visualization of the tumor expressing RFP. Under the GFP filter, both AlexaFluor 488- and the RFP-expressing tumor are simultaneously visualized, giving a *yellow color*. The high correlation of *red* and *green* indicates high specificity of the green fluorophore-labeled anti-CEA antibody
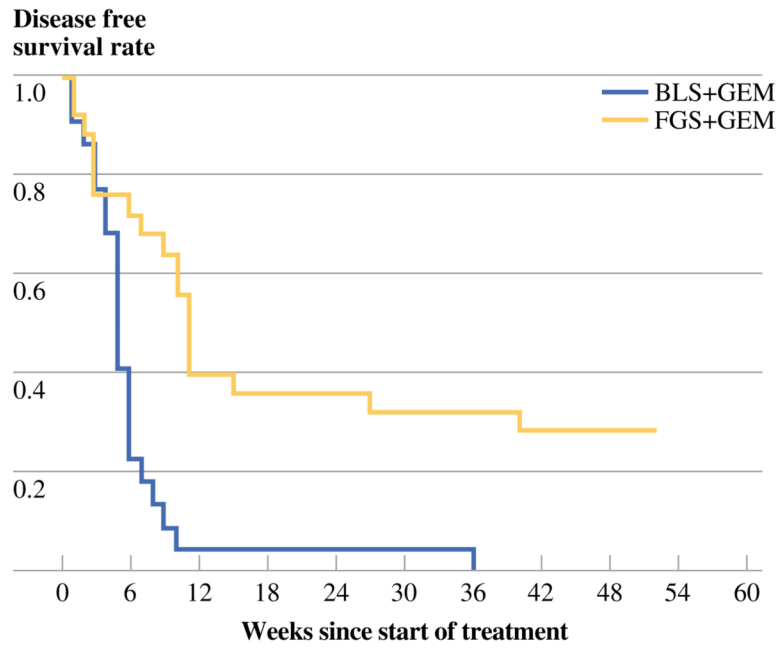
Fig. 3.

Disease-free survival (DFS). There was a significant difference in DFS between the 2 surgical groups ($p < 0.0001$). Mice in the FGS group had a median DFS of 11 weeks compared to 5 weeks in the BLS group. Tumor never regressed in the other two treatment groups, and they were therefore excluded from this plot
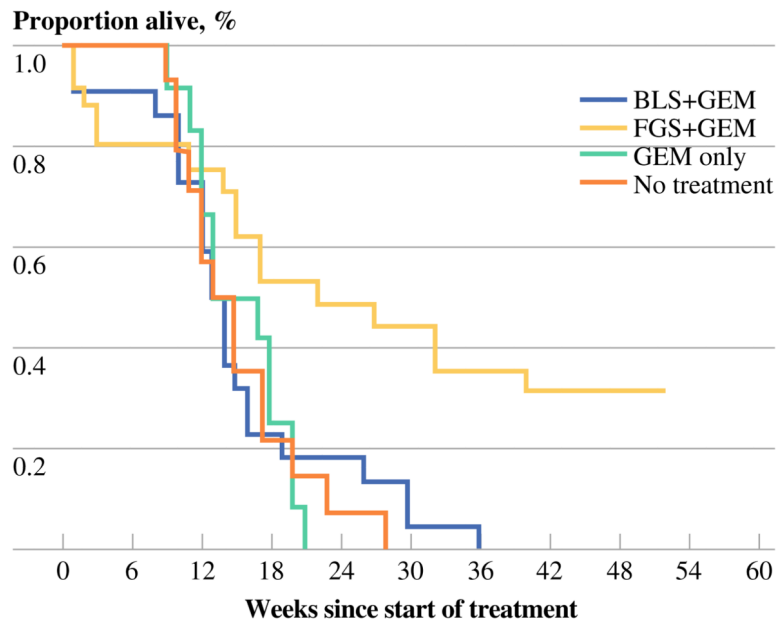
Fig. 4.
Overall survival (OS). OS did not significantly differ between the control group, the GEM-only group, and the BLS+GEM group. However, FGS+GEM significantly lengthened OS in the mouse models of human pancreatic cancer ($p = 0.003$)

Table 1

Outcomes by surgical method

Surgical method	F0 resection rate	Cure rate	1-year survival rate[a]
BLS+GEM	10/22 (45.5 %)	1/22 (4.5 %)	0/21 (0 %)
FGS+GEM	23/25 (92 %)	10/25 (40 %)	7/25 (28 %)
p value	0.001	0.01	0.01

F0 is defined as the absence of fluorescence signal in the postsurgical bed on postoperative images obtained with the OV-100 Small Animal Imaging System under the GFP filter; cure was defined by the absence of tumor at time of death or termination as long as the mouse survived longer than 12 weeks postoperatively

BLS bright-light surgery, *GEM* gemcitabine, *FGS* fluorescence-guided surgery

[a]Two mice in the FGS+GEM group went missing at 10 weeks and so did not have a death status available at 1 year; these animals were counted as dead